

Forced expression of DNA methyltransferases during oocyte growth accelerates the establishment of methylation imprints but not functional genomic imprinting

Satoshi Hara, Takashi Takano, Tsugunari Fujikawa, Munehiro Yamada, Takuya Wakai, Tomohiro Kono and Yayoi Obata*

Department of BioScience, Tokyo University of Agriculture, 1-1-1 Sakuragaoka, Setagaya-ku, Tokyo 156-8502, Japan

Received September 28, 2013; Revised January 27, 2014; Accepted March 3, 2014

In mammals, genomic imprinting governed by DNA methyltransferase DNMT3A and its cofactor DNMT3L is essential for functional gametes. Oocyte-specific methylation imprints are established during oocyte growth concomitant with DNMT3A/DNMT3L expression, although the mechanisms of oocyte-specific imprinting are not fully understood. To determine whether the presence of DNMT3A/DNMT3L in oocytes is sufficient for acquisition of methylation imprints, we produced transgenic mice to induce DNMT3A/DNMT3L expression prematurely in oogenesis and analyzed DNA methylation imprints. The results showed that 2- to 4-fold greater expression of DNMT3A/DNMT3L was achieved in non-growing (ng) oocytes versus fully grown oocytes derived from wild-type mice, but the analyzed imprint domains were not methylated. Thus, the presence of DNMT3A/DNMT3L in ng oocytes is insufficient for methylation imprints, and imprinted regions are resistant to DNMT3A/DNMT3L in ng oocytes. In contrast, excess DNMT3A/DNMT3L accelerated imprint acquisition at *Igf2r*, *Lit1*, *Zac1* and *Impact* but not *Snrpn* and *Mest* in growing oocytes. Therefore, DNMT3A/DNMT3L quantity is an important factor for imprint acquisition. Transcription at imprinted domains is proposed to be involved in *de novo* methylation; however, transcription at *Lit1*, *Snrpn* and *Impact* was observed in ng oocytes. Thus, transcription cannot induce DNMT3A catalysis at imprinted regions even if DNMT3A/DNMT3L is present. However, the accelerated methylation imprints in oocytes, with the exception of *Igf2r*, were erased during embryogenesis. In conclusion, a sufficient amount of DNMT3A/DNMT3L and a shift from the resistant to permissive state are essential to establish oocyte-specific methylation imprints and that maintenance of the acquired DNA methylation imprints is essential for functional imprinting.

INTRODUCTION

In mammals, uniparental embryos that contain only maternal or paternal genomes die shortly after implantation due to gamete-specific epigenetic modifications, genomic imprinting, which leads to parent-of-origin-specific gene expression during embryogenesis (1,2). Embryos lacking genomic imprinting cannot achieve normal ontogeny (3,4). Therefore, the establishment of genomic imprinting is essential to produce functional gametes (5).

A major molecular mechanism for genomic imprinting is methylation of cytosine residues in CpG dinucleotides. Imprinted domains contain differentially methylated regions (DMRs) between the maternal and paternal alleles that are inherited from the oocytes and sperm (6,7). Embryos in which the DMRs are disrupted do not exhibit allele-specific gene expression; thus, the maintenance of DMRs in somatic cell lineages is essential for regulated expression of imprinted genes (8–13). DMR methylation is erased from the germ cell lineage to

*To whom correspondence should be addressed at: Department of BioScience, Tokyo University of Agriculture, 1-1-1 Sakuragaoka, Setagaya-ku, Tokyo 156-8502, Japan. Tel: +81 354772755; Fax: +81 354772755; Email y1obata@nodai.ac.jp

reprogram parentally derived imprinting (14,15). *De novo* DNA methylation occurs to establish genomic imprinting based on individual sex (16–19). Twenty-two DMRs have been identified; 19 of them are methylated in oogenesis and the remainder are methylated in spermatogenesis (14).

DNA methyltransferase (DNMT), DNMT3A, and its non-enzymatic cofactor DNMT3L (DNMTs) are indispensable for DNA methylation imprints during gametogenesis (20–22). Deletion of *Dnmt3a* or *Dnmt3L* in oocytes prevents oocyte-specific methylation imprints and the resultant embryos cannot develop beyond mid-gestational stage due to abnormal expression of imprinted genes (23,24). Furthermore, *Dnmt3a* and *Dnmt3L* co-expression is not observed in non-growing (ng) oocytes but expression levels increase with oocyte growth (25). Oocyte-specific methylation imprints are absent in ng oocytes and are gradually imposed on growing oocytes with gene-specific timing until they are full grown (fg) (3,18); hypermethylation is achieved for *Igf2r*, *Lit1* and *Zac1* in mid-growing oocytes and for *Snrpn*, *Impact* and *Mest* in late-growth oocytes (3,17,18,26). Thus, co-expression of *Dnmt3a* and *Dnmt3L* coincides with acquisition of methylation imprints.

Recently, additional factors have been found to be essential for DNA methylation imprints during oogenesis. Ciccone *et al.* showed that *Kdm1b* coding histone H3 lysine 4 (H3K4) demethylase is required for DNA methylation imprints at *Grb10*, *Mest*, *Zac1* and *Impact* but not *Igf2r*, *Lit1* and *Snrpn* (27). This suggests that KDM1B controls imprinting of those genes that acquire DNA methylation imprints relatively late during oocyte growth. Transcription through DMRs at *Snrpn* and *Gnas* was observed in growing oocytes, and transcript truncation upstream of the DMRs led to a loss of DNA methylation at these loci (28,29). However, KDM1B and transcription through DMRs account for genomic imprinting at defined regions and are not common to most imprinted regions. This raises the question of whether the presence of DNMT3A and DNMT3L in oocytes is sufficient for acquisition of DNA methylation imprints at least in some regions, i.e. does excess DNMTs expression accelerate imprinting acquisition in oocytes. To address this question, we analyzed DNA methylation and transcription at imprinted domains in transgenic (Tg) mice in which DNMT3A and DNMT3L expression in oocytes is induced prior to endogenous DNMTs expression.

RESULTS

Expression of DNMT3A and DNMT3L in oocytes

Dnmt3a contains *Dnmt3a2*, a short isoform produced from an alternative promoter; however, it is unclear which type of DNMT3A is expressed in mouse oocytes. We examined the expression of DNMT3A, DNMT3A2 and DNMT3L during oogenesis in 100 oocytes (Fig. 1). Western blotting showed no DNMT3A expression, whereas the absolute level of DNMT3A2 expression increased with oocyte growth. DNMT3L was not detected in oocytes with a diameter of 40–49 μm but was detected at low levels in oocytes with a diameter of 50–59 μm ; it was most strongly expressed in fg oocytes. DNMT3A, DNMT3A2 and DNMT3L were not detected in ng oocytes. These results indicate that DNMT3A2 but not DNMT3A is

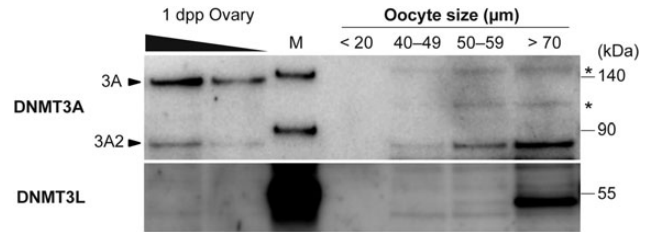


Figure 1. Western blotting of endogenous DNMT3A and DNMT3L in oocytes derived from WT mice. Ovarian samples derived from newborn mice were diluted to 50% (left) and 25% (right). One hundred oocytes were pooled according to their diameter: <20, 40–49, 50–59 and >70 μm . These were electrophoresed and treated with the anti-DNMT3A antibody, recognizing DNMT3A and DNMT3A2, and anti-DNMT3L antibody. Ovarian samples indicate quantitative detection. DNMT3A; 130 kDa, DNMT3A2; 85 kDa, DNMT3L; 50 kDa, M; molecular weight marker and asterisk; non-targeted bands indicated by the molecular weight marker.

predominately expressed in oocytes during establishment of methylation imprints.

Production of *Dnmt3a2/Dnmt3L* conditional Tg mice

As shown in Figure 1, neither DNMT3A2 nor DNMT3L were detected in ng oocytes. To investigate whether the absence of methylation imprints in ng oocytes is due to a lack of DNMT3A2 and DNMT3L, we produced *Dnmt3a2* and *Dnmt3L* conditional Tg mice by using the Cre/loxP system. The Tg vector was designed to induce EGFP expression ubiquitously in Tg mice harboring the 2lox allele and to induce *mCherry*, *Dnmt3a2* and *Dnmt3L* expression only in the 1lox allele by Cre-mediated recombination (Fig. 2A). Tg copy number was assessed by Southern blotting and two of four 2lox Tg lines that harbored 5–10 copies (lines ak and q) were used for further study (Supplementary Material, Fig. S1). These 2lox(+) female mice were crossed with male *Vasa-Cre*(+) Tg mice. As expected, the floxed-EGFP cassette was removed concomitantly with the induction of robust *mCherry* expression in 1lox oocytes derived from double Tg [2lox(+)/*Vasa-Cre*(+)] embryos beginning 15.5 days postcoitum (dpc) (Fig. 2B; Supplementary Material, Fig. S2). Quantitative RT-PCR (qRT-PCR) showed that *Dnmt3a* and *Dnmt3L* expression was significantly higher in 1lox ng oocytes derived from double Tg [2lox(+)/*Vasa-Cre*(+)] mice than in 2lox and naive ng oocytes derived from 2lox(+)/*Vasa-Cre*(–) and wild-type (WT) littermates (Fig. 2C). Expression levels in 1lox ng oocytes were equal to or greater than those in WT fg oocytes and male germ cells in which methylation imprints are established at 16.5 dpc (Fig. 2C). Western blotting showed that DNMT3A2 and DNMT3L were weakly or not expressed in the neonatal ovaries of 2lox(+)/*Vasa-Cre*(–) and WT siblings, whereas DNMT3A2 and DNMT3L were strongly expressed in the neonatal ovaries of double Tg [2lox(+)/*Vasa-Cre*(+)] mice (Fig. 2D). To confirm that DNMT3A2 and DNMT3L were derived from 1lox ng oocytes, western blot analysis was conducted in the oocytes (Fig. 2E). Result showed that relative expression levels of DNMT3A2 and DNMT3L in 1lox ng oocytes were 1.4- to 2.3- and 2.2- to 4.0-fold higher than in WT fg oocytes. Thus, Tg mice that show induction of sufficient DNMT3A2 and DNMT3L expression in ng oocytes were successfully produced.

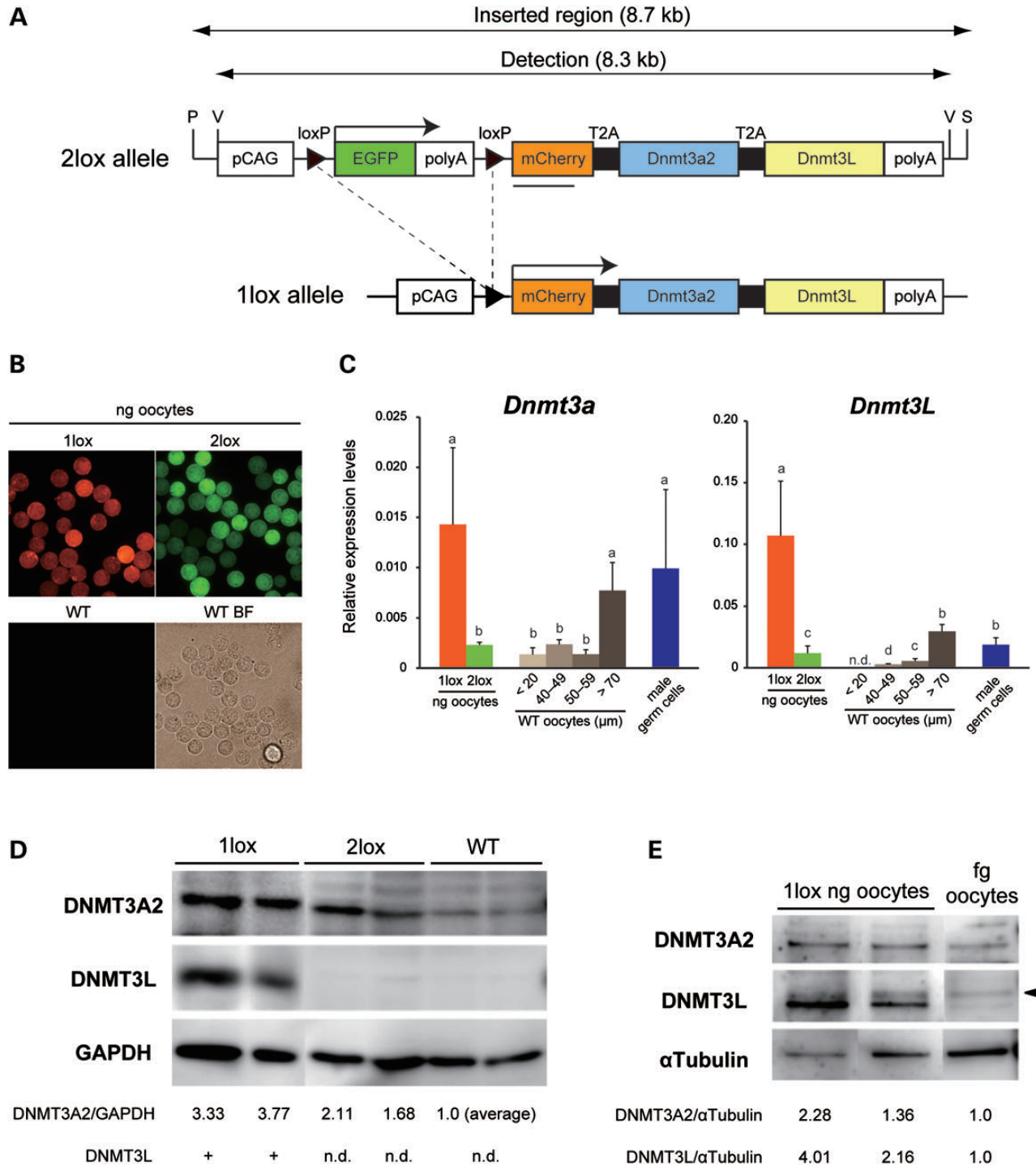


Figure 2. Generation of *Dnmt3a2* and *Dnmt3L* conditional Tg mice. (A) Schematic representation of the conditional Tg allele. 2lox vector (upper) is designed to express only EGFP but not the downstream sequences from the chicken beta-actin promoter (pCAG). The floxed-EGFP cassette is removed in the presence of Cre recombinase, concomitantly with the induction of *mCherry*, *Dnmt3a2* and *Dnmt3L*, all linked by T2A peptides, in the 1lox allele (lower). Tg mice were generated by microinjection of linearized 2lox vector (8.7 kb) by double digestion of *Psp1406I* (P) and *SfiI* (S). *VspI* (V) digestion was used for Southern hybridization. (B) Expression of the immunofluorescence reporters mCherry and EGFP in 1lox and 2lox ng oocytes, respectively. mCherry expression was not observed in 2lox ng oocytes. (C) qRT-PCR of *Dnmt3a*, detecting *Dnmt3a* and *Dnmt3a2*, and *Dnmt3L* in 1lox (orange bar) and 2lox (green bar) ng oocytes, various sizes of WT oocytes (brown bars) and WT male germ cells derived from 16.5 dpc embryos (blue bar). Error bars represent standard deviation. Relative expression in 1lox ng oocytes was equal to or greater than in oocytes and male germ cells during imprinting establishment. A different letter over the bar represents a significant difference ($P < 0.05$). (D) Western blotting of DNMT3A2 and DNMT3L in the newborn ovary from double [2lox(+)/Vasa-Cre(+)], 2lox [2lox(+)/Vasa-Cre(-)] and WT mice. The relative DNMT levels are shown. (E) Western blotting of DNMT3A2 and DNMT3L in 1lox ng oocytes from double Tg [2lox(+)/Vasa-Cre(+)] and fg oocytes from WT mice.

DNA methylation imprints in 1lox ng oocytes

DNA methylation at imprinted loci was analyzed in 1lox ng oocytes derived from double Tg [2lox(+)/Vasa-Cre(+)] mice by sodium bisulfite sequencing. Controls were 2lox ng oocytes derived from 2lox(+)/Vasa-Cre(-) littermates. The 1lox ng oocytes, similar to 2lox ng oocytes, were free of DNA methylation at *Zac1*, *Impact* and *Mest* DMRs, which acquire KDM1B-dependent imprints during oocyte growth (Fig. 3A); this suggests ng oocytes lack KDM1B. We then examined *Igf2r*, *Lit1* and *Snrpn* DMRs, which acquire KDM1B-independent imprints during oocyte growth; we also examined *Peg3* DMR. DNA methylation analysis showed that *Lit1*, *Snrpn* and *Peg3* DMRs were not methylated in 1lox ng oocytes as they were in 2lox ng oocytes (Fig. 3B). With one exception, *Igf2r* DMR was methylated but only partially in 1lox ng oocytes (1lox versus 2lox, 20.0 versus 0.8%). The methylation levels of 1lox ng oocytes were equivalent to those of 2lox ng oocytes at *Igf2/H19* DMR, which is imprinted during spermatogenesis, and at endogenous retroviral elements IAP (Fig. 3C). Thus, the presence of DNMT3A2 and DNMT3L in ng oocytes is not sufficient for DNA methylation imprints regardless of KDM1B dependency; i.e. most DMRs are resistant to DNMTs in ng oocytes.

Acceleration of DNA methylation imprints in 1lox oocytes

All imprinted regions should be released from their DNMTs-resistant state at some point during oocyte growth. Next, we investigated whether imprinting acquisition accelerates in 1lox growing oocytes with a sufficient amount of DNMTs. Western blotting showed that slightly higher levels of DNMT3A2 and 3-fold higher levels of DNMT3L accumulated prematurely in 1lox oocytes than in 2lox and WT oocytes (Figs 2C and 4A). DNA methylation levels in *Igf2r* and *Lit1* DMRs increased in 1lox growing oocytes in comparison with 2lox growing oocytes with a diameter of 40–49 μm (*Igf2r*, 1lox versus 2lox, 77 versus 24%, $P < 0.001$; *Lit1*, 1lox versus 2lox, 56 versus 20%; $P < 0.05$). The *Snrpn* DMR showed equivalent methylation levels in 1lox and 2lox growing oocytes with a diameter of 40–49 μm (49 versus 39%). Complete methylation at the *Zac1* DMR was observed in 1lox growing oocytes but not in 2lox growing oocytes with a diameter of 40–49 μm (92 versus 29%; $P < 0.001$). *Impact* and *Mest* DMRs, imprinting of which depends on the KDM1B as well as *Zac1* DMR, were partially methylated but still exhibited hypomethylation in 1lox growing oocytes with a diameter of 40–49 μm (*Impact*, 1lox versus 2lox, 29 versus 15%; *Mest*, 1lox versus 2lox, 12 versus 1%; $P < 0.001$) (Fig. 4B; Supplementary Material, Fig. S3). Almost complete methylation imprints were established at *Igf2r* and *Lit1* DMRs in 1lox growing oocytes with a diameter of 50–59 μm . This was accelerated in comparison with the progression of methylation imprints in 2lox growing oocytes of the same size (Fig. 4B; Supplementary Material, Fig. S3). However, there were no significant differences in the methylation levels of *Snrpn* DMR between 1lox and 2lox growing oocytes of this size (71 versus 65%). The *Impact* DMR began to undergo *de novo* methylation at a higher rate in 1lox than in 2lox growing oocytes with a diameter of 50–59 μm (85 versus 24%), but the *Mest* DMR remained comparably hypomethylated (1lox versus 2lox, 30 versus 13%; $P = 0.052$) (Fig. 4B; Supplementary

Material, Fig. S3). Thus, excess DNMTs accelerated imprint acquisition in *Igf2r*, *Lit1*, *Zac1* and *Impact* but not *Snrpn* and *Mest*, which suggests gene-specific timing.

To confirm that accelerated DNA methylation in 1lox growing oocytes was dependent on the amount of DNMTs, we analyzed another Tg line (p) that harbored a lower copy number (3–5 copies) than lines ak and q (Supplementary Material, Fig. S4). DNA methylation of *Igf2r* DMR was significantly higher in 1lox than in 2lox growing oocytes even in line p (40–49 μm ; 51 versus 14%, 50–59 μm ; 94 versus 65%; $P < 0.001$); however, this level was significantly lower in line p than in line ak (40–49 μm ; 51 versus 77%; $P < 0.001$). This strongly suggests that the amount of DNMTs is associated with accelerated methylation acquisition.

Transcription across DMR during oogenesis

To address the question of why DNMT3A2 cannot catalyze *de novo* methylation at most DMRs in ng oocytes and whether the transition of DMRs from DNMTs-resistance to -permissiveness is associated with transcription, we examined transcription across DMR in various sizes of oocytes. RT-PCR revealed *Kcnq1*, *Snrpn* and *Impact* transcripts in oocytes of every size, including ng oocytes, whereas *Igf2r*, *Zac1* and *Mest* transcripts were detected only in oocytes $>40 \mu\text{m}$ (Fig. 5A). As in WT oocytes, these results were confirmed in 1lox and 2lox oocytes (Fig. 5B). Transcripts across DMRs were observed in oocytes when DNA methylation imprints were established; however, transcriptional activation does not always correspond with the shift of DMRs from resistant to permissive for DNMTs.

Function of accelerated DNA methylation imprints

We determine whether the accelerated methylation imprints during oocyte growth contribute to functional imprinting in embryogenesis, i.e. can regulate imprinted expression. To do this, we generated fertilized eggs that contained the genome from 1lox growing oocytes with a diameter of 50–59 μm by nuclear transfer (1lox-NT). Then, DNA methylation and mRNA expression at several imprinted loci were analyzed in 9.5 dpc embryos. Biparental embryos harboring the genome from WT fg (fg-NT) or WT growing oocytes with a diameter of 50–59 μm (WT-NT) were used as control. Hypomethylation, partial methylation and hypermethylation were judged as methylation of $\leq 10\%$, 10–90% and $\geq 90\%$ of the analyzed CpG sites in a DNA strand. In WT-NT embryo, mosaicism of hyper- and hypomethylation was observed in *Igf2r* and *Zac1* maternal alleles (Fig. 6A). Maternal *Lit1*, *Impact* and *Mest* DMRs were completely hypomethylated in WT-NT embryos. Consistent with their methylation status, *Igf2r* and *p57^{kip2}* were repressed presumably due to *Air* and *Lit1* expression and *Mest* and *Impact* were overexpressed in comparison with fg-NT embryos (Fig. 6B). Unexpectedly, *Zac1* was downregulated in WT-NT embryo. In contrast, in all of the 1lox-NT embryos, the maternal *Igf2r* alleles were hypermethylated, whereas maternal *Lit1* alleles were hypomethylated. Mosaicism of DNA methylation was observed at *Zac1*, *Impact* and *Mest* maternal alleles. *Impact* and *Mest* maternal alleles were hypomethylated in two of three 1lox-NT embryos (Fig. 6A). qRT-PCR showed that *Igf2r* mRNA expression was restored to

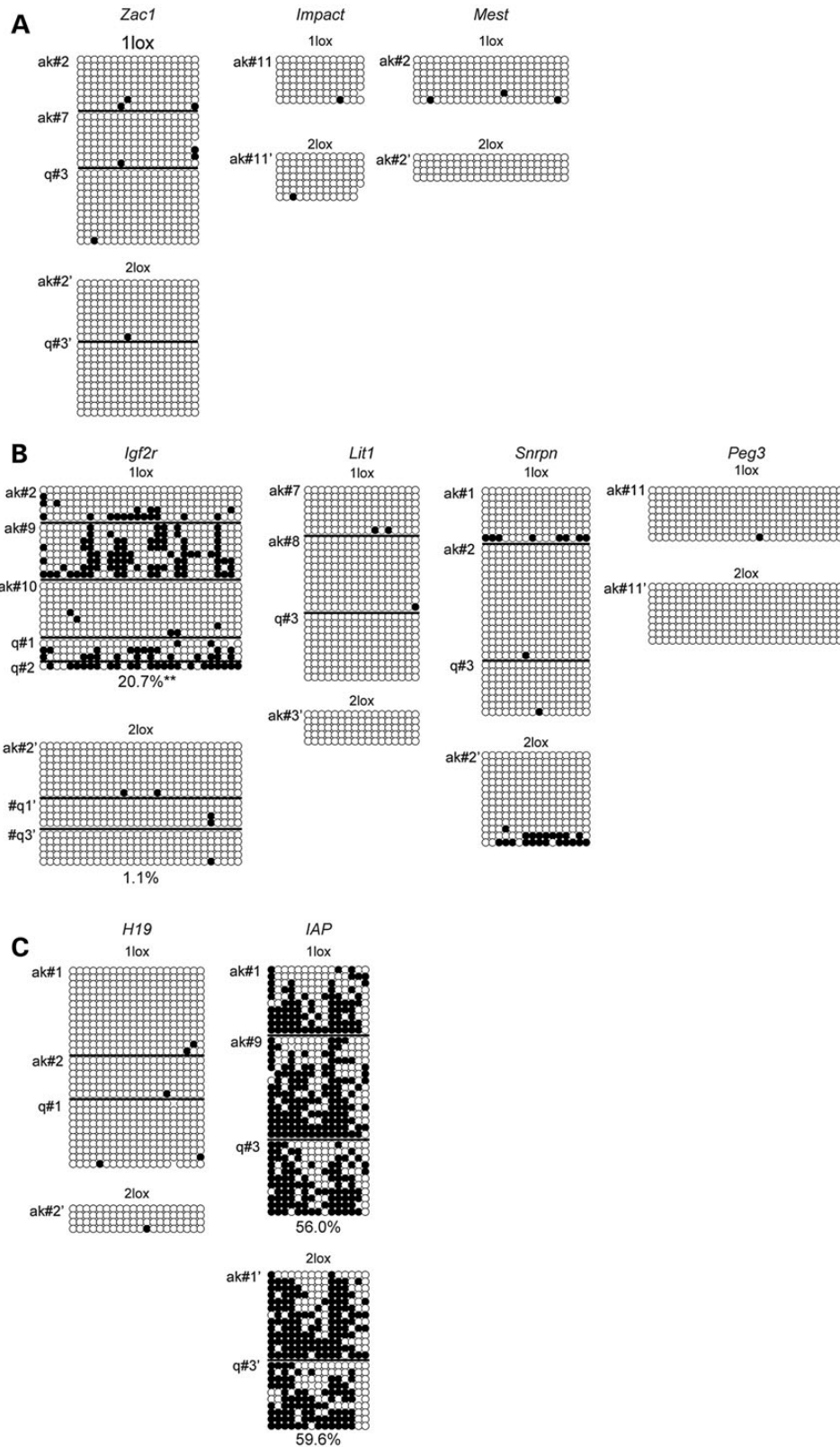
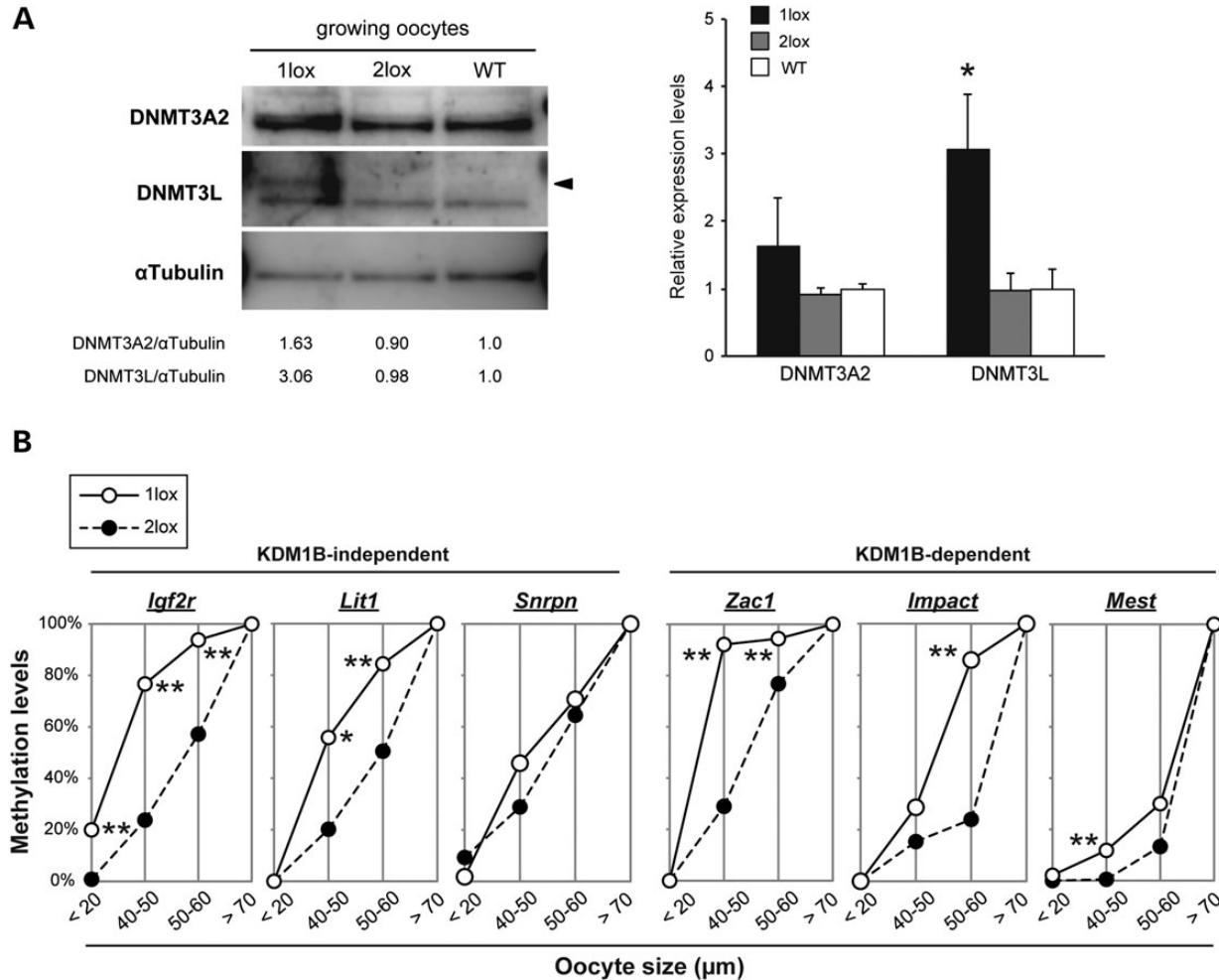


Figure 3. DNA methylation status at imprinted loci in 1lox and 2lox ng oocytes. DNA methylation analyses of DMRs methylated during oocyte growth in a KDM1B-dependent (**A**) and -independent (**B**) manner; *H19* DMR is methylated in spermatogenesis, and retroviral repeated sequence IAP (**C**). Unmethylated and methylated CpG sites are represented by open and filled circles, respectively. Each line of circles indicates one DNA strand. The horizontal line indicates data derived from individual Tg mice. Two asterisks represent significant differences between 1lox and 2lox oocytes ($P < 0.01$).



normal levels but *p57^{kip2}* was repressed in all 1lox-NT embryos. *Zac1*, *Impact* and *Mest* were not overexpressed, inconsistent with their methylation status (Fig. 6B). Developmental ability of 1lox-NT embryos was lower than in fg-NT embryos (21 versus 57%) at 9.5 dpc (Supplementary Material, Table S1). We did not observe a dramatic restoration of developmental ability in 1lox-NT embryos. Thus, accelerated methylation imprints during oocyte growth cannot serve as functional imprinting in embryogenesis, with the exception of *Igf2r* DMR.

DISCUSSION

The N-terminally truncated DNMT3A isoform DNMT3A2 is expressed in male germ cells during the late gestational period when sperm-specific DNA methylation imprints are established (30). O'Doherty *et al.* showed that DNMT3A and DNMT3A2 are similarly expressed in bovine oocytes (31). However, we found that DNMT3A2 is predominately expressed in mouse oocytes during the growth phase, suggesting DNMT3A2 is responsible for DNA methylation imprints in female germ

lines as well as male. Furthermore, western blotting showed a gradual increase in oocyte DNMT3A2 expression during the growth phase, while DNMT3L was not detectable in oocytes $< 50 \mu\text{m}$. We and others have reported complete methylation of *Igf2r*, *Lit1* and *Zac1* DMRs in WT growing oocytes with a diameter of 55–59 μm (13). Thus, DNMT3L expression coincided with increasing levels of DNA methylation at *Igf2r*, *Lit1* and *Zac1* DMRs in WT oocytes (Fig. 7). This is consistent with earlier suggestions that DNMT3L mediates enzymatic activation or recruitment of DNMT3A2 (32,33).

To understand the molecular mechanisms of genomic imprinting, we investigated whether the presence of DNMT3A2 and DNMT3L in oocytes is sufficient for acquisition of DNA methylation imprints; in other words, is the absence of methylation imprints in ng oocytes due to a lack of DNMT3A2 and DNMT3L. Previous reports have shown that expression of *Dnmt3a* and *Dnmt3L* peaks in fg oocytes and male germ cells of 16.5 dpc embryos (25,30). Compared with these cells, *Dnmt3a2* mRNA was expressed at the same level and *Dnmt3L* mRNA was 5-fold higher in 1lox ng oocytes. DNMT3A2 and DNMT3L proteins were 1.4- to 2.3- and 2.2- to 4.0-fold higher

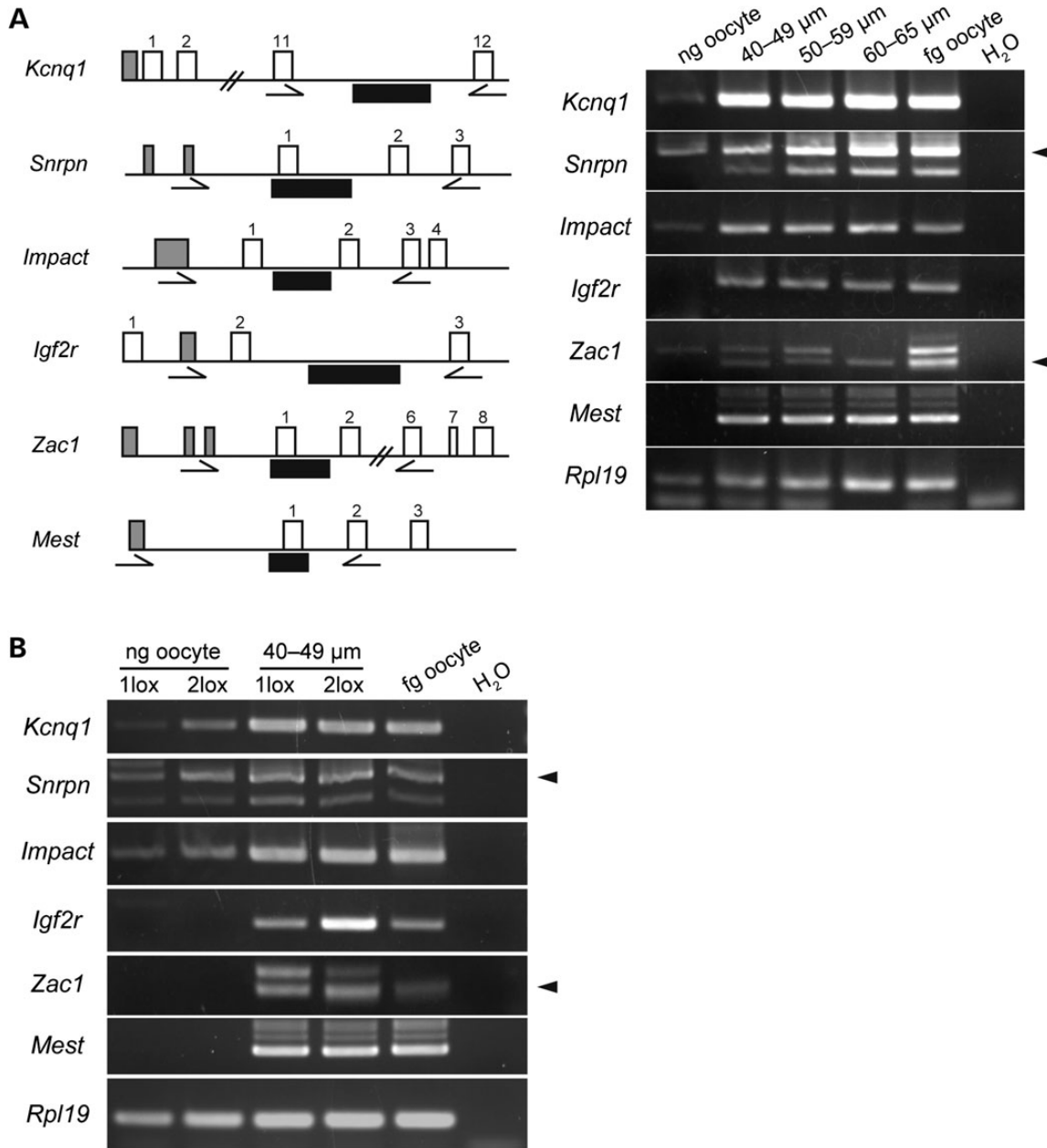


Figure 5. Detection of transcripts across DMRs by RT-PCR. (A) Schematic diagram (left panel) showing transcripts across *Snrpn*, *Kcnq1* (*Lit1*), *Impact*, *Igf2r*, *Zac1* and *Mest* DMRs and agarose gel images (right panel) showing transcripts in WT oocytes during growth. Somatic exons, oocyte-specific exons and DMRs are represented by open, gray and black boxes, respectively. Arrows and arrowheads indicate primers for RT-PCR analyses and target transcripts, respectively. *Rpl19* was used as an internal control. (B) Agarose gel images showing transcripts across DMRs in 1lox and 2lox oocytes at ng and early growing stage. Transcripts were observed in 1lox and 2lox oocytes.

than in WT fg oocytes. In this study, expression levels of the DNMTs mRNA and protein varied in 1lox ng oocytes. We observed that both of EGFP and mCherry were positive in ng oocytes whereas only mCherry was positive in fg oocytes derived from double Tg [2lox(+)/Vasa-Cre(+)] mice (paper has been submitted). Therefore, this is likely due to the efficiency of *Vasa*-driven Cre recombination in multiple 2lox transgenes at the ng stage. DNMT3A2 and DNMT3L in 1lox ng oocytes were assumed sufficient to catalyze *de novo* methylation. Nevertheless, methylation imprints were not established at all the loci analyzed

in 1lox ng oocytes. This finding clearly showed that DNMT3A2 and DNMT3L are insufficient for establishment of methylation imprints and imprinted loci are substantially resistant to DNMTs in ng oocytes. DNMT3L interacts specifically with unmethylated histone H3K4 in *in vitro* interaction assays (34–36). KDM1B, a demethylase of histone H3K4, is required to establish DNA methylation imprints at some loci but not at *Igf2r*, *Lit1* and *Snrpn*. It is unclear whether another enzyme catalyzes demethylation of H3K4 at *Igf2r*, *Lit1* and *Snrpn*. Our results showed that hypermethylation did not occur at *Igf2r*, *Lit1* and

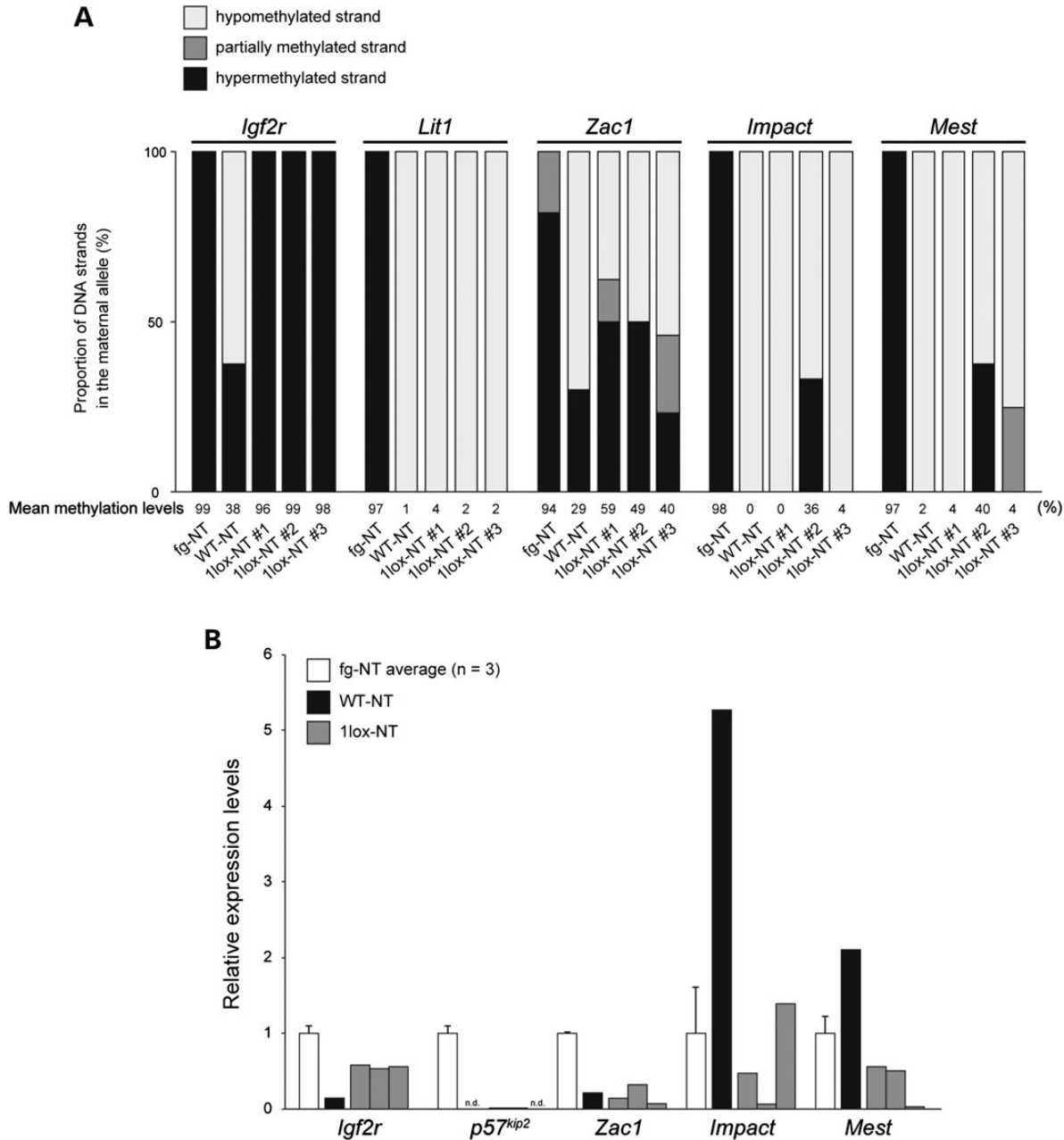


Figure 6. DNA methylation and expression of imprinted genes in 1lox-NT embryos at 9.5 dpc. **(A)** DNA methylation analysis at DMRs in 1lox-NT embryos. The methylation imprint is judged to be hypomethylated, partially methylated or hypermethylated strand when $\leq 10\%$, $10\text{--}90\%$ or $\geq 90\%$, respectively, of the analyzed CpG sites in a DNA strand are methylated. Bars indicate the proportion of DNA strands in the maternal allele at each DMR. Parental alleles were discriminated by DNA polymorphisms between lab mouse (C57BL/6 or FVB) and JF1. Data from three individual 1lox-NT embryos are shown (#1; 20–25 somite stage, #2; 20–25 somite stage, #3; 15–20 somite stage). All of the fg-NT embryos were at the 25–30 somite stage and WT-NT embryo was at the 20–25 somite stage. **(B)** qRT-PCR analysis of imprinted genes in 1lox-NT embryos. The mRNA levels of maternally expressed *Igf2r* and *p57^{kip2}* and paternally expressed *Zac1*, *Impact* and *Mest* were normalized to *Gapdh*. Bars indicate expression levels relative to that of fg-NT embryos. Error bars indicate standard deviation. Data from three individual 1lox-NT embryos are shown.

Snrpn loci in 1lox ng oocytes. Therefore, other factors must be required for the shift from DNMTs-resistant to -permissive states at KDM1B-independent DMRs (Fig. 7).

Recently, we found that long exposure of ng nuclei to fg ooplasm induced DNMT3A and DNMT3L expression and partial DNA methylation at *Igf2r*, *Lit1* and unexpectedly *H19* DMRs (37). We speculated that *de novo* DNA methylation at

imprinted loci in the ng oocyte genome was driven by DNMTs in nuclear transferred oocytes and that certain factors protecting *H19* DMR against DNMTs might be absent in the ng oocyte genome. Partial methylation at the *Igf2r* DMR in nuclear transferred oocytes was consistent with the present data. However, *Lit1* and *H19* DMRs were not methylated in 1lox ng oocytes. We now speculate that partial methylation at *Igf2r*, *Lit1* and

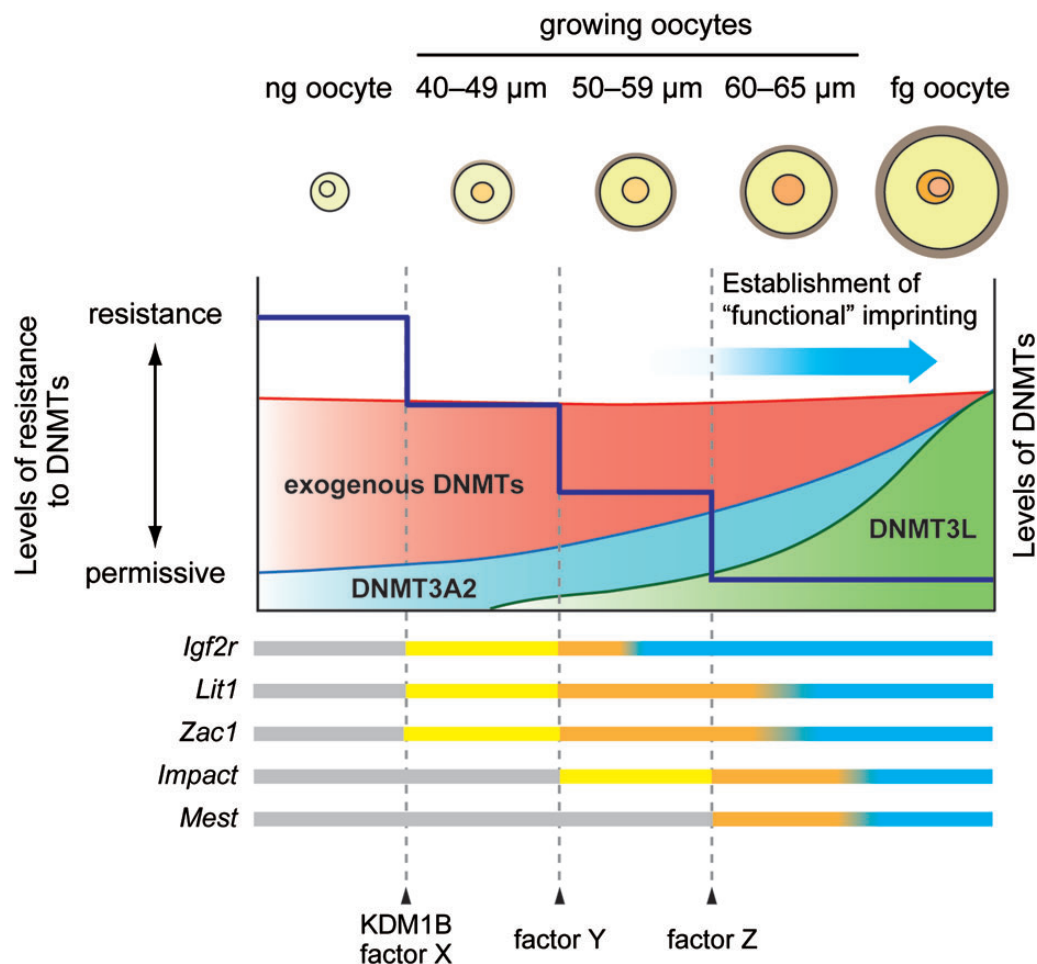


Figure 7. Schematic diagram of the oocyte-specific methylation imprints and putative chromatin states at each DMR. Endogenous DNMT3A2 and DNMT3L are shown as blue and green shading, respectively. Exogenous DNMT3A2 and DNMT3L are shown in red. The shift from resistant to permissive chromatin state for DNMTs is represented by a dark blue line. Factors (X, Y, Z and so on) are necessary for this transition. Gray bars indicate that 10–30% of the CpG sites are methylated in DMRs. Yellow (1lox) and orange (WT) bars indicate that >50% of the CpG sites are methylated in DMR. Blue bars indicate establishment of functional imprinting.

H19 DMRs in nuclear transferred oocytes is due to reactivation of DNMTs and altered sensitivity to DNMTs via chromatin remodeling on the ng oocyte genome.

We also examined whether imprinting acquisition accelerates in 1lox growing oocytes with a sufficient amount of DNMTs. The results showed that *Igf2r*, *Lit1* and *Zac1* DMRs reached much higher levels of DNA methylation in 1lox oocytes than in WT and 2lox oocytes with a diameter of 40–49 μm . Advanced methylation imprint in 1lox oocytes with a diameter of 50–59 μm was seen in *Impact* DMR. This accelerated methylation imprinting is due to large amounts of exogenous DNMTs. Thus, the quantity of DNMTs is an important factor for imprint acquisition. Furthermore, the permissive state for DNMTs extends to *Igf2r*, *Lit1* and *Zac1* DMRs in early growing stage and to *Impact* DMR in the middle growing stage prior to the accumulation of the necessary amount of endogenous DNMTs in WT oocytes. Most interestingly, KDM1B-dependent DMRs *Zac1*, *Impact* and *Mest* showed different patterns of progression of DNA methylation in 1lox oocytes; *Mest* persists in hypomethylation. These findings suggest gene-specific timing for imprint acquisition is modulated by mechanisms that

control the shift from the resistant to the permissive chromatin state. Unknown factor(s) in addition to KDM1B must regulate extension of the permissive state for DNMTs in *Impact* and *Mest* DMRs (Fig. 7).

Genome-wide DNA methylomes and transcriptomes have been reported (38). DNA methylation preferentially occurs in active transcription units. As well as imprinted loci, transcription across DMRs including oocyte-specific exons was identified in oocytes during methylation establishment (28), although transcription in ng oocytes was not analyzed. Furthermore, truncating transcripts through DMRs in oocytes disrupts oocyte-derived DMR methylation at *Snrpn* and *Gnas* in the resultant embryos (28,29). These results lead us to hypothesize that transcription across DMRs changes the chromatin state to become permissive for DNMTs. Here, we analyzed transcription across DMRs in various sizes of oocytes to understand whether the transition from DNMTs-resistant to -permissive is associated with transcriptional activation. Unexpectedly, transcription at *Igf2r*, which was partially methylated in 1lox ng oocytes, was not observed in 1lox ng oocytes. Transcripts across each DMR at *Lit1*, *Snrpn* and *Impact* were detected in 1lox ng oocytes;

however, methylation of these DMRs was absent in 1lox ng oocytes. Our data indicate that transcription through DMRs did not play a primary role in changing from the resistant to the permissive state at most DMRs.

Finally, we investigated whether accelerated methylation imprints in 1lox growing oocytes can be functional. Our previous study showed that embryos containing a maternal genome derived from growing oocytes exhibit frequently epigenetic mosaicism or a loss of methylation imprint (LOM) at maternal alleles during embryogenesis (13). In this study, accelerated methylation imprints in 1lox growing oocytes were not disrupted at *Igf2r* DMR but resulted in LOM at *Lit1* DMR and epigenetic mosaicism at *Zac1* and *Impact* DMRs in 1lox-NT embryos. The most likely explanation for LOM and epigenetic mosaicism is that epigenetic modification such as dimethylation of histone H3K9 would be absent or incomplete in the genome of growing oocytes. Previously, Nakamura *et al.* demonstrated that protection against DNA demethylation at maternal DMRs after fertilization was achieved by PGC7 and H3K9 dimethylation (39,40). Human maternal hypomethylation syndrome, in which LOM occurs at multiple maternal loci, is an imprinting disorder. DNMT3L and/or DNMT1 deletions were not detected but the ZFP57 mutation was detected in patients (41,42). Therefore, the effect of ZFP57 on DMRs during oocyte growth is key to functional imprinting. Alternatively, DNMTs-permissive state is reminiscent of relaxed chromatin conformation so DMRs might change again DNMTs-permissive to -resistant state after imprint acquisition. In contrast, *Zac1*, *Impact* and *Mest* were not overexpressed in 1lox-NT embryos in spite of LOM at maternal alleles. Rather, their expression levels were slightly low than in fg-NT embryos. The reason for this discrepancy is unclear, but the same phenomenon was observed previously (13). The developmental rate of 1lox-NT embryos was not much higher than that of WT-NT embryos (Supplementary Material, Table S1). This is consistent with the fact that acquired methylation imprints were erased during embryogenesis.

In this study, we revealed that the presence of DNMT3A2 and DNMT3L in ng oocytes is not sufficient for methylation imprints. However, forced expression of DNMT3A2 and DNMT3L accelerated the establishment of methylation imprints during oocyte growth at four of six tested DMRs. Unique patterns of imprint acquisition are mediated by DNMTs quantity and gene-specific molecules such as KDM1B (27), ZFP57 (43) and unknown factors, which are essential for changing DMRs to the permissive chromatin status for DNMTs. However, accelerated methylation imprints cannot be maintained during embryogenesis, with the exception of *Igf2r* DMR. To understand the mechanisms of functional genomic imprinting and to elucidate the etiology of maternal hypomethylation syndrome, we must investigate histone modification or chromatin structure in oocytes.

MATERIALS AND METHODS

Ethics

All procedures were reviewed and approved by the Tokyo University of Agriculture Institutional Animal Care and Use Committee and were performed in accordance with the

Guidelines for Proper Conduct of Animal Experiments, as established by the Science Council of Japan.

Generation of Tg mice

Tg mice harboring floxed-EGFP allele (2lox mice) were generated by microinjection of vectors linearized using *Psp1406I* and *SfiI* (Takara Bio, Tokyo, Japan) into the paternal pronucleus of C57BL/6N-background zygotes (Fig. 2A) (44). The copy number of Tg in each line of 2lox mice was determined by Southern blotting. DNA extracted from 2lox mouse tails was treated with *VspI* (New England Biolabs Japan, Tokyo, Japan) and hybridized with DIG-labelled DNA probes synthesized with the DIG PCR Synthesis Kit (Roche Diagnostics Japan, Tokyo, Japan).

To produce conditional Tg mice in which DNMT3A2 and DNMT3L expression is induced during gametogenesis, female 2lox mice were crossed with FVB-background Vasa-Cre male mice (purchased from the Jackson Laboratory, Maine, USA) (45), and double Tg mice containing both 2lox and Vasa-Cre alleles were generated. Genotypes were verified by PCR with primers specific for EGFP, *Dnmt3a2*, *Dnmt3L* and *Cre* (Supplementary Material, Table S2).

Oocyte collection

ng and growing oocytes were collected from newborn (0–2 days postpartum; dpp) and 10–15 dpp female mice. Ovaries were treated with 0.1% collagenase in L-15 medium for 40 min and 0.05% trypsin–0.53 mM EDTA in PBS for 15 min at 37°C. ng oocytes and ovarian somatic cells were suspended in M2 medium containing 5 µg/ml cytochalasin B (Sigma-Aldrich Japan, Tokyo, Japan) and the oocytes were isolated with a micromanipulator. Growing oocytes were treated with 0.5% Pronase (Sigma-Aldrich) in L-15 medium for 15 min at 37°C to remove zona and somatic cells were completely removed by pipetting. Oocyte diameters were measured and growing oocytes in M2 medium containing 240 µM dibutyryl cyclic AMP (Sigma-Aldrich) were sorted by size (40–49, 50–59 and 60–65 µm in diameter) with a micromanipulator under an interference microscope (OLYMPUS, Tokyo, Japan) with a CCD camera (Keyence, Osaka, Japan). fg oocytes were obtained from the ovaries of 8- to 12-week-old adult mice at 44–46 h after injection with 5 IU equine chorionic gonadotropin (eCG; serotropin; ASKA Pharmaceutical Company, Tokyo, Japan). Cumulus cell-oocyte complexes were isolated and cumulus cells were completely removed by pipetting.

Production of biparental embryos from growing oocytes by nuclear transfer

Adult BDF1 (C57BL/6N × DBA/2 hybrid; CLEA Japan, Tokyo, Japan) female mice were injected with 5 IU eCG, and 5 IU human chorionic gonadotropin (hCG; Puberogen; Yell Pharmaceutical, Tokyo, Japan) was injected 48 h after the eCG injection. fg oocytes were collected at the germinal vesicle stage as described above. Freshly ovulated oocytes at the second meiosis were collected from the oviducts 14–16 h after the hCG injection. Serial nuclear transfers were performed as previously described (13). Sperm were collected from JF1

male mice (*Mus musculus molossinus*) (46), and the reconstituted oocytes by serial nuclear transfer were incubated with sperm for 6 h in TYH medium (47). The resulting blastocysts were transferred to the uterine horns of pseudopregnant female mice at 2.5 dpc. Embryos were dissected at 9.5 dpc. Each embryo was divided into two pieces to assess the DNA methylation and mRNA expression of imprinted genes.

DNA methylation analysis

For DNA methylation analysis, 400–500 ng oocytes and 150–200 growing oocytes were pooled and incubated in 18 μ l lysis buffer (1% SDS, 5 μ g Proteinase K and 2 μ g of *Escherichia coli* tRNA) for 1 h at 37°C. Embryos were lysed in HMW buffer (10 mM Tris–HCl (pH 8.0), 50 mM NaCl, 5 mM EDTA and 0.1% SDS) at 55°C for 12 h and subjected to phenol-chloroform extraction. DNA samples were treated with EpiTect Bisulfite (Qiagen, Tokyo, Japan) for sodium bisulfite conversion. One to five independent samples were analyzed (Fig. 3; Supplementary Material, Figs S3 and S4). Bisulfite-treated DNA, the equivalent of 50 oocytes, was subjected to nested PCR. PCR products were cloned into pGEM-T easy (Promega, Tokyo, Japan), and >20 clones were sequenced on an Applied Bioscience sequencing system (ABI PRISM 3100, Applied Bioscience; LifeScience Technologies Japan, Tokyo, Japan). Differences in DNA methylation levels were assessed using QUMA (48) with Mann–Whitney *U* test. DNA methylation data were analyzed only when the bisulfite conversion rate was >95%. Primers for nested PCR are listed in Supplementary Material, Table S2 and previous reports (13,18).

Western blotting

Ovaries from 1 dpp female mice, 2000 ng oocytes and 100 oocytes of each size were washed in PBS containing 0.1% polyvinyl alcohol and lysed in sample buffer (0.25 M Tris–HCl (pH 6.8), 40% glycerol, 0.8% SDS and 1% β -mercaptoethanol). Proteins were separated by SDS–PAGE in 5–20% gradient gels (ATTO, Tokyo, Japan) and transferred to PVDF membranes. Blocking and immunoreactions were performed with the Can Get Signal Immunoreaction Kit (TOYOBO, Osaka, Japan) and the following antibodies: anti-Dnmt3a (IMGEX, IMG-268A, CA, USA; 1:2000), anti-Dnmt3L (gifted from Shoji Tajima, 1:2000), anti-GAPDH (Trevigen, Gaithersburg, UK, 1:2000) and anti- α -tubulin (Sigma-Aldrich, 1:2000). Western blot experiments were repeated at least three times.

mRNA expression analysis

Total RNA from oocytes was isolated with the RNeasy Micro Kit (Qiagen). RNA quality was assessed by using the Agilent 2100 Bioanalyzer and RNA 6000 Pico Chip.

To conduct qRT-PCR, total RNA was isolated from 400 ng oocytes, 400 male germ cells derived from 16.5 dpc embryos, 150–200 growing oocytes, 80–100 fg oocytes and each embryo. In the case of germ cells, cDNA was synthesized by PrimeScript (Takara Bio) from total RNA by using oligo d(T) primer. cDNA from embryos was synthesized from 1 μ g total RNA. qRT-PCR for *Dnmt3a*, *Dnmt3L*, *Igf2r*, *p57^{kip2}*, *Zac1*, *Impact* and *Mest* was performed on a 7500 Real-Time System (Applied

Bioscience) with the following TaqMan probes: *Dnmt3a* (detection of *Dnmt3a* and *Dnmt3a2*), Mm00432876_m1; *Dnmt3L*, Mm00457635_m1; *Igf2r*, Mm00439576_m1; *p57^{kip2}*, Mm00494251_m1; *Zac1*, Mm00438170_m1; *Impact*, Mm00492647_m1; *Mest*, Mm00484993_m1 and *Gapdh*, Mm99999915_g1. Gene expression was evaluated relative to *Gapdh* in individual samples. Three independent samples were analyzed.

To detect transcription across DMRs, 5 ng total RNA was isolated from 1500 to 2000 ng oocytes, 150 to 200 growing oocytes and 80 to 100 fg oocytes. cDNA was synthesized with SuperScript III and random primers. RT-PCR was performed with Ex Taq Hot Start Version (Takara Bio) and the primers listed in Supplementary Material, Table S2 under standard conditions. Transcripts across DMR were confirmed by sequencing the PCR products.

SUPPLEMENTARY MATERIAL

Supplementary Material is available at *HMG* online.

ACKNOWLEDGEMENTS

We thank Prof. Shoji Tajima (Osaka University) for providing the anti-DNMT3L antibody, Prof. Izuhito Hatada and Dr Sumiyu Morita (Gunma University) for providing the DNMT3L cDNA clone, Profs Hiroyuki Sasaki and Andras Nagy for providing TNAP-Cre mouse, and Prof. Masahito Ikawa (Osaka University), Dr Hajime Matsubara (Tokyo University of Agriculture) and Dr Kazuhiko Nakabayashi (National Research Institute for Child Health and Development, Japan) for helpful comments.

Conflict of Interest statement. None declared.

FUNDING

This work was supported in part by the Naito Foundation and Grants-in-Aid for Scientific Research 23616006 and 25114008 to Y.O. Funding to pay the Open Access publication charges for this article was provided by the Naito Foundation to Y.O.

REFERENCES

- Sotomaru, Y., Katsuzawa, Y., Hatada, I., Obata, Y., Sasaki, H. and Kono, T. (2002) Unregulated expression of the imprinted genes H19 and *Igf2r* in mouse uniparental fetuses. *J. Biol. Chem.*, **277**, 12474–12478.
- Ogawa, H., Wu, Q., Komiyama, J., Obata, Y. and Kono, T. (2006) Disruption of parental-specific expression of imprinted genes in uniparental fetuses. *FEBS Lett.*, **580**, 5377–5384.
- Kono, T., Obata, Y., Yoshimizu, T., Nakahara, T. and Carroll, J. (1996) Epigenetic modifications during oocyte growth correlates with extended parthenogenetic development in the mouse. *Nat. Genet.*, **13**, 91–94.
- Obata, Y., Kaneko-Ishino, T., Koide, T., Takai, Y., Ueda, T., Domeki, I., Shiroishi, T., Ishino, F. and Kono, T. (1998) Disruption of primary imprinting during oocyte growth leads to the modified expression of imprinted genes during embryogenesis. *Development*, **125**, 1553–1560.
- Sasaki, H. and Matsui, Y. (2008) Epigenetic events in mammalian germ-cell development: reprogramming and beyond. *Nat. Rev. Genet.*, **9**, 129–140.
- Ferguson-Smith, A.C., Sasaki, H., Cattanch, B.M. and Surani, M.A. (1993) Parental-origin-specific epigenetic modification of the mouse H19 gene. *Nature*, **362**, 751–755.
- Stoger, R., Kubicka, P., Liu, C.G., Kafri, T., Razin, A., Cedar, H. and Barlow, D.P. (1993) Maternal-specific methylation of the imprinted mouse *Igf2r*

- locus identifies the expressed locus as carrying the imprinting signal. *Cell*, **73**, 61–71.
8. Li, E., Beard, C. and Jaenisch, R. (1993) Role for DNA methylation in genomic imprinting. *Nature*, **366**, 362–365.
 9. Birger, Y., Shemer, R., Perk, J. and Razin, A. (1999) The imprinting box of the mouse *Igf2r* gene. *Nature*, **397**, 84–88.
 10. Fitzpatrick, G.V., Soloway, P.D. and Higgins, M.J. (2002) Regional loss of imprinting and growth deficiency in mice with a targeted deletion of *KvDMR1*. *Nat. Genet.*, **32**, 426–431.
 11. Lin, S.P., Youngson, N., Takada, S., Seitz, H., Reik, W., Paulsen, M., Cavaille, J. and Ferguson-Smith, A.C. (2003) Asymmetric regulation of imprinting on the maternal and paternal chromosomes at the *Dlk1-Gtl2* imprinted cluster on mouse chromosome 12. *Nat. Genet.*, **35**, 97–102.
 12. Williamson, C.M., Turner, M.D., Ball, S.T., Nottingham, W.T., Glenister, P., Fray, M., Tymowska-Lalanne, Z., Plagge, A., Powles-Glover, N., Kelsey, G. *et al.* (2006) Identification of an imprinting control region affecting the expression of all transcripts in the *GNAS* cluster. *Nat. Genet.*, **38**, 350–355.
 13. Obata, Y., Hiura, H., Fukuda, A., Komiya, J., Hatada, I. and Kono, T. (2011) Epigenetically immature oocytes lead to loss of imprinting during embryogenesis. *J. Reprod. Dev.*, **57**, 327–334.
 14. Kobayashi, H., Sakurai, T., Miura, F., Imai, M., Mochiduki, K., Yanagisawa, E., Sakashita, A., Wakai, T., Suzuki, Y., Ito, T. *et al.* (2013) High-resolution DNA methylome analysis of primordial germ cells identifies gender-specific programming in mice. *Genome Res.*, **23**, 616–627.
 15. Lee, J., Inoue, K., Ono, R., Ogonuki, N., Kohda, T., Kaneko-Ishino, T., Ogura, A. and Ishino, F. (2002) Erasing genomic imprinting memory in mouse clone embryos produced from day 11.5 primordial germ cells. *Development*, **129**, 1807–1817.
 16. Davis, T.L., Yang, G.J., McCarrey, J.R. and Bartolomei, M.S. (2000) The H19 methylation imprint is erased and re-established differentially on the parental alleles during male germ cell development. *Hum. Mol. Genet.*, **9**, 2885–2894.
 17. Obata, Y. and Kono, T. (2002) Maternal primary imprinting is established at a specific time for each gene throughout oocyte growth. *J. Biol. Chem.*, **277**, 5285–5289.
 18. Hiura, H., Obata, Y., Komiya, J., Shirai, M. and Kono, T. (2006) Oocyte growth-dependent progression of maternal imprinting in mice. *Genes Cells*, **11**, 353–361.
 19. Li, J.Y., Lees-Murdock, D.J., Xu, G.L. and Walsh, C.P. (2004) Timing of establishment of paternal methylation imprints in the mouse. *Genomics*, **84**, 952–960.
 20. Okano, M., Bell, D.W., Haber, D.A. and Li, E. (1999) DNA methyltransferases *Dnmt3a* and *Dnmt3b* are essential for de novo methylation and mammalian development. *Cell*, **99**, 247–257.
 21. Bourc'his, D., Xu, G.L., Lin, C.S., Bollman, B. and Bestor, T.H. (2001) *Dnmt3L* and the establishment of maternal genomic imprints. *Science*, **294**, 2536–2539.
 22. Kaneda, M., Okano, M., Hata, K., Sado, T., Tsujimoto, N., Li, E. and Sasaki, H. (2004) Essential role for de novo DNA methyltransferase *Dnmt3a* in paternal and maternal imprinting. *Nature*, **429**, 900–903.
 23. Hata, K., Okano, M., Lei, H. and Li, E. (2002) *Dnmt3L* cooperates with the *Dnmt3* family of de novo DNA methyltransferases to establish maternal imprints in mice. *Development*, **129**, 1983–1993.
 24. Kaneda, M., Hirasawa, R., Chiba, H., Okano, M., Li, E. and Sasaki, H. (2010) Genetic evidence for *Dnmt3a*-dependent imprinting during oocyte growth obtained by conditional knockout with *Zp3-Cre* and complete exclusion of *Dnmt3b* by chimera formation. *Genes Cells*, **15**, 169–179.
 25. Lucifero, D., La Salle, S., Bourc'his, D., Martel, J., Bestor, T.H. and Trasler, J.M. (2007) Coordinate regulation of DNA methyltransferase expression during oogenesis. *BMC Dev. Biol.*, **7**, 36.
 26. Lucifero, D., Mann, M.R., Bartolomei, M.S. and Trasler, J.M. (2004) Gene-specific timing and epigenetic memory in oocyte imprinting. *Hum. Mol. Genet.*, **13**, 839–849.
 27. Ciccone, D.N., Su, H., Hevi, S., Gay, F., Lei, H., Bajko, J., Xu, G., Li, E. and Chen, T. (2009) *KDM1B* is a histone H3K4 demethylase required to establish maternal genomic imprints. *Nature*, **461**, 415–418.
 28. Chotalia, M., Smallwood, S.A., Ruf, N., Dawson, C., Lucifero, D., Frontera, M., James, K., Dean, W. and Kelsey, G. (2009) Transcription is required for establishment of germline methylation marks at imprinted genes. *Genes Dev.*, **23**, 105–117.
 29. Smith, E.Y., Futtner, C.R., Chamberlain, S.J., Johnstone, K.A. and Resnick, J.L. (2011) Transcription is required to establish maternal imprinting at the Prader-Willi syndrome and Angelman syndrome locus. *PLoS Genet.*, **7**, e1002422.
 30. Sakai, Y., Suetake, I., Shinozaki, F., Yamashina, S. and Tajima, S. (2004) Co-expression of de novo DNA methyltransferases *Dnmt3a2* and *Dnmt3L* in gonocytes of mouse embryos. *Gene Expr. Patterns*, **5**, 231–237.
 31. O'Doherty, A.M., O'Shea, L.C. and Fair, T. (2012) Bovine DNA methylation imprints are established in an oocyte size-specific manner, which are coordinated with the expression of the *DNMT3* family proteins. *Biol. Reprod.*, **86**, 1–10.
 32. Chedin, F., Lieber, M.R. and Hsieh, C.L. (2002) The DNA methyltransferase-like protein *DNMT3L* stimulates de novo methylation by *Dnmt3a*. *Proc. Natl. Acad. Sci. USA*, **99**, 16916–16921.
 33. Suetake, I., Morimoto, Y., Fuchikami, T., Abe, K. and Tajima, S. (2006) Stimulation effect of *Dnmt3L* on the DNA methylation activity of *Dnmt3a2*. *J. Biochem.*, **140**, 553–559.
 34. Jia, D., Jurkowska, R.Z., Zhang, X., Jeltsch, A. and Cheng, X. (2007) Structure of *Dnmt3a* bound to *Dnmt3L* suggests a model for de novo DNA methylation. *Nature*, **449**, 248–251.
 35. Ooi, S.K., Qiu, C., Bernstein, E., Li, K., Jia, D., Yang, Z., Erdjument-Bromage, H., Tempst, P., Lin, S.P., Allis, C.D. *et al.* (2007) *DNMT3L* connects unmethylated lysine 4 of histone H3 to de novo methylation of DNA. *Nature*, **448**, 714–717.
 36. Li, B.Z., Huang, Z., Cui, Q.Y., Song, X.H., Du, L., Jeltsch, A., Chen, P., Li, G., Li, E. and Xu, G.L. (2011) Histone tails regulate DNA methylation by allosterically activating de novo methyltransferase. *Cell Res.*, **21**, 1172–1181.
 37. Obata, Y., Wakai, T., Hara, S. and Kono, T. (2014) Long exposure to mature ooplasm can alter DNA methylation at imprinted loci in non-growing oocytes but not in prospermatogonia. *Reproduction*, **147**, H1–H6.
 38. Kobayashi, H., Sakurai, T., Imai, M., Takahashi, N., Fukuda, A., Yayoi, O., Sato, S., Nakabayashi, K., Hata, K., Sotomaru, Y. *et al.* (2012) Contribution of intragenic DNA methylation in mouse gametic DNA methylomes to establish oocyte-specific heritable marks. *PLoS Genet.*, **8**, e1002440.
 39. Nakamura, T., Arai, Y., Umehara, H., Masuhara, M., Kimura, T., Taniguchi, H., Sekimoto, T., Ikawa, M., Yoneda, Y., Okabe, M. *et al.* (2007) *PGC7/Stella* protects against DNA demethylation in early embryogenesis. *Nat. Cell Biol.*, **9**, 64–71.
 40. Nakamura, T., Liu, Y.J., Nakashima, H., Umehara, H., Inoue, K., Matoba, S., Tachibana, M., Ogura, A., Shinkai, Y. and Nakano, T. (2012) *PGC7* binds histone H3K9me2 to protect against conversion of 5mC to 5hmC in early embryos. *Nature*, **486**, 415–419.
 41. Azzi, S., Rossignol, S., Steunou, V., Sas, T., Thibaud, N., Danton, F., Le Jule, M., Heinrichs, C., Cabrol, S., Gicquel, C. *et al.* (2009) Multilocus methylation analysis in a large cohort of 11p15-related foetal growth disorders (Russell Silver and Beckwith Wiedemann syndromes) reveals simultaneous loss of methylation at paternal and maternal imprinted loci. *Hum. Mol. Genet.*, **18**, 4724–4733.
 42. Mackay, D.J., Callaway, J.L., Marks, S.M., White, H.E., Acerini, C.L., Boonen, S.E., Dayanikli, P., Firth, H.V., Goodship, J.A., Haemers, A.P. *et al.* (2008) Hypomethylation of multiple imprinted loci in individuals with transient neonatal diabetes is associated with mutations in *ZFP57*. *Nat. Genet.*, **40**, 949–951.
 43. Li, X., Ito, M., Zhou, F., Youngson, N., Zuo, X., Leder, P. and Ferguson-Smith, A.C. (2008) A maternal-zygotic effect gene, *Zfp57*, maintains both maternal and paternal imprints. *Dev. Cell*, **15**, 547–557.
 44. Okabe, M., Ikawa, M., Kominami, K., Nakanishi, T. and Nishimune, Y. (1997) 'Green mice' as a source of ubiquitous green cells. *FEBS Lett.*, **407**, 313–319.
 45. Gallardo, T., Shirley, L., John, G.B. and Castrillon, D.H. (2007) Generation of a germ cell-specific mouse transgenic *Cre* line, *Vasa-Cre*. *Genesis*, **45**, 413–417.
 46. Koide, T., Moriwaki, K., Uchida, K., Mita, A., Sagai, T., Yonekawa, H., Katoh, H., Miyashita, N., Tsuchiya, K., Nielsen, T.J. *et al.* (1998) A new inbred strain *JF1* established from Japanese fancy mouse carrying the *classic piebald* allele. *Mamm. Genome*, **9**, 15–19.
 47. Toyoda, Y., Yokoyama, M. and Hoshi, T. (1971) Studies on the fertilization of mouse eggs in vitro I: In vitro fertilization of eggs by fresh epididymal sperm. *Jpn. J. Anim. Reprod.*, **16**, 147–151.
 48. Kumaki, Y., Oda, M. and Okano, M. (2008) QUMA: quantification tool for methylation analysis. *Nucleic Acids Res.*, **36**, W170–W175.